Second-generation stoichiometric mathematical model to predict methane emissions from oil sands tailings

Jude D. Kong [a,b], Hao Wang [b,*], Tariq Siddique [c], Julia Foght [d], Kathleen Semple [d], Zvonko Burkus [e], Mark A. Lewis [b,d]

[a] Center for Discrete Mathematics and Theoretical Computer Science, Rutgers University, 96 Frelinghuysen Road Piscataway, NJ 08854-8018, USA
[b] Department of Mathematical and Statistical Sciences, University of Alberta, Edmonton, AB T6G 2G1, Canada
[c] Department of Renewable Resources, University of Alberta, Edmonton, AB T6G 2G7, Canada
[d] Department of Biological Sciences, University of Alberta, Edmonton, AB T6G 2E9, Canada
[e] Alberta Environment and Parks, Government of Alberta, Edmonton, Canada

HIGHLIGHTS

- Native microbes anaerobically biodegrade diluent hydrocarbons in tailings ponds.
- Fugitive diluent in tailings is a significant biogenic methane (CH_4) source.
- About 40% mass of naphtha and 60% mass of paraffinic diluent are biodegradable.
- Mathematical model is developed for CH_4 biogenesis from hydrocarbon biodegradation.
- About 50–75% of CH_4 emissions in-situ are due to diluent biodegradation.

GRAPHICAL ABSTRACT
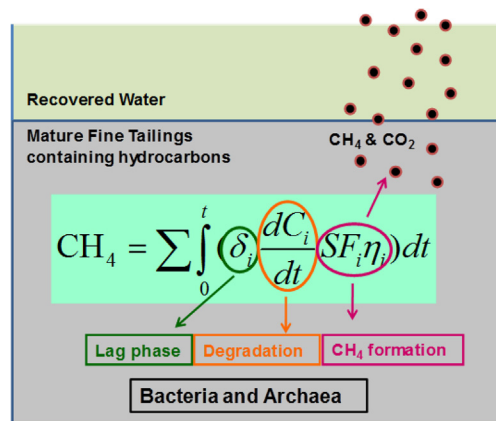
$$CH_4 = \sum \int_0^t \left(\delta_i \frac{dC_i}{dt} SF_i \eta_i \right) dt$$

ABSTRACT

Microbial metabolism of fugitive hydrocarbons produces greenhouse gas (GHG) emissions from oil sands tailings ponds (OSTP) and end pit lakes (EPL) that retain fluid tailings from surface mining of oil sands ores. Predicting GHG production, particularly methane (CH_4), would help oil sands operators mitigate tailings emissions and may assist regulators evaluating the trajectory of reclamation scenarios. Using empirical datasets from laboratory incubation of OSTP sediments with pertinent hydrocarbons, we developed a stoichiometric model for CH_4 generation by indigenous microbes. This model improved on previous first-approximation models by considering long-term biodegradation kinetics for 18 relevant hydrocarbons from three different oil sands operations, lag times, nutrient limitations, and microbial growth and death rates. Laboratory measurements were used to estimate model parameter values and to validate the new model. Goodness of fit analysis showed that the stoichiometric model predicted CH_4 production well; normalized mean square error analysis revealed that it surpassed previous models. Comparison of model predictions with field measurements of CH_4 emissions further validated the new model. Importantly, the

* Corresponding author.
  E-mail address: hao8@ualberta.ca (H. Wang).

Oil sands tailings pond
End pit lake

model also identified in-situ parameters that are currently lacking but are needed to enable future robust modeling of CH_4 production from OSTP and EPL in-situ.

1. Introduction

Alberta's oil sands industry is a major economic driver in Canada, currently producing ~3 million barrels oil d^{-1} and expected to reach 4 million barrels d^{-1} by 2024 (Government of Alberta, 2019; AER, 2019a). However, the oil sands sector (colloquially also known as "tar sands") has come under international scrutiny regarding GHG emissions and other environmental issues. Oil sands operations including mining, upgrading and in-situ extraction were responsible for ~43% of Alberta's overall GHG emissions in 2012 (Alberta Greenhouse Gas Report, 2016). In addition to these production operations, the storage and management of aqueous slurries of surface-mined ore processing wastes in oil sands tailings ponds (OSTP; Fig. S1) contributes substantially to methane (CH_4) and carbon dioxide (CO_2) emissions (Burkus et al., 2014; Siddique et al., 2008). Total fugitive GHG emissions from major oil sands operators' OSTP, measured in-situ using floating flux chambers in 2011, were calculated to be 2.8 million tonnes CO_2 equivalent per year (Burkus et al., 2014), while in 2018 they were estimated at ~2.2 Mt. of CO_2e (Z. Burkus, unpublished). Furthermore, proposed implementation of EPL as a long-term reclamation strategy for OSTP sediments (Fig. S1) may contribute additional GHG emissions for an unknown timespan.

During five decades of retention, enormous volumes of tailings have accumulated that are currently estimated at >1.26 billion m^3 (AER, 2019b) As the fluid tailings in OSTP age, the suspended clay fines settle via several physical and biogeochemical mechanisms including gravity and porewater and solid phase chemistry (Siddique et al., 2014) to become anaerobic mature fine tailings (MFT) that have a solids content >30 wt% and possess both an active microbiota and residual diluent in progressive stages of selective biodegradation (Fig. S2 in Foght et al., 2017). The use of EPL has been discussed to reintegrate the accumulated tailings into the on-site environment (Charette et al., 2012) and proposed by industry in their tailings management plans as one of their closure approaches (AER, 2019a, 2019b). In this reclamation scenario, after years or decades of residence in OSTP, MFT would be treated and transported to mined-out pits and capped with fresh water and/or process-affected water. This is intended to establish a sustainable aquatic system (i.e., an end pit lake; EPL) that, with time, should support economic, ecological and/or societal uses (Charette et al., 2012). However, ebullition of GHG from underlying sediments may delay EPL ecosystem development by dispersing fine sediments into the overlying water layer and potentially co-transporting some constituents of concern. Thus, GHG emissions from oil sands tailings repositories are problematic from global warming as well as ecological standpoints.

GHG emissions from OSTP and EPL result primarily from anaerobic biodegradation of diluent hydrocarbons (naphtha or light paraffins) introduced into tailings after aqueous extraction of bitumen from oil sands ore and treatment of froth (Fig. S1; reviewed in Foght et al., 2017). The diluents, specific to each operator, facilitate separation of bitumen from water and mineral solid particles during froth treatment and reduce bitumen viscosity in preparation for processing and/or transport. Most of the diluent is recovered from the froth treatment tailings for re-use, but a small proportion remains in the tailings slurry that comprises alkaline water, sand, silt, clays and unrecovered bitumen. These fresh tailings, as well as other tailings streams that have not been exposed to diluent, are deposited in OSTP where indigenous anaerobic microbial communities oxidize the labile (biodegradable) hydrocarbons to CH_4 and CO_2 (Abu Laban et al., 2015; Penner and Foght, 2010; Mohamad Shahimin et al., 2016; Siddique et al., 2011). Although naphtha and paraffinic diluents are considered to be the major carbon sources for microbes in OSTP (Foght et al., 2017), only certain of their hydrocarbon components are known to be biodegradable under anaerobic conditions, whereas others are recalcitrant (slowly or incompletely biodegraded) or are completely resistant to biodegradation (Siddique et al., 2018). Although bitumen is the overwhelming organic constituent of fresh tailings, it predominantly comprises recalcitrant hydrocarbons: only a small proportion may be biodegradable and the contribution of bitumen to biogenic GHG is thought to be negligible in proportion to that of diluent (Foght et al., 2017).

The importance of modeling GHG emissions is clear to oil sands operators, as it provides a rationale for mitigating GHG mitigation efforts and managing OSTP and EPL. However, field data (e.g., concentrations of individual hydrocarbons in OSTP, nutrient concentrations, biomass) needed for modeling are generally unavailable either because collection of such data is technologically difficult or because such key model parameters have not previously been identified as necessary. Therefore, we have incubated MFT in laboratory cultures analogous to OSTP and EPL for use in initial modeling efforts. A previous study (Siddique et al., 2008) used limited data available from short-term (<1 yr) laboratory studies measuring biodegradation of a small subset of components (Siddique et al., 2007, 2006) in a single naphtha diluent to develop zero- and first-order kinetic models for estimating CH_4 production potential from a single OSTP. That first approximation model predicted in-situ CH_4 production volumes reasonably consistent with emissions measured in-situ (Siddique et al., 2008). However, in the decade since that work, additional components of naphtha and paraffinic diluent have been shown to support methanogenesis from MFT during extended laboratory incubation (up to 6.5 y; Abu Laban et al., 2015; Mohamad Shahimin et al., 2016; Siddique et al., 2015, 2011). This finding increases theoretical GHG emissions, especially from hydrocarbons previously assumed to be recalcitrant and thus not considered in the previous model and over extended time scales more relevant to long-term retention of tailings. Moreover, data are now available for additional OSTP receiving different diluents and therefore having unique microbial communities (Wilson et al., 2016) with different CH_4 production potentials, and the effect of potentially growth-limiting nutrients in-situ such as nitrogen has begun to be examined (Collins et al., 2016). Also, the first EPL field trial was established in 2013 where CH_4 has been detected within the water cap (Risacher et al., 2018). The greatly expanded data set and a broader understanding of oil sands tailings microbiology (Foght et al., 2017) enable and have driven development of the improved and flexible model for CH_4 generation described here.

The goals of the new stoichiometric model were: (1) to expand CH_4 predictive capability by considering methanogenic biodegradation of a wider range of hydrocarbons only recently shown to be labile over longer incubation times; (2) to include OSTP that receive diluents having different compositions and that harbour different microbial communities; (3) to account for the effects of nutrient limitation on CH_4 generation, particularly available nitrogen; (4) to compare model predictions with field measurements of CH_4 emissions to validate the model and reveal any shortcomings; (5) to consider differences in GHG emission trajectories between OSTP and EPL; and (6) to identify parameters essential for future development of a model to predict CH_4 emissions in-situ in OSTP and EPL.

2. Materials and methods

Although the gaseous products of methanogenic hydrocarbon biodegradation are CH_4 and CO_2 (Fig. S2), the stoichiometric model developed here considers only CH_4 production for two reasons: CH_4 has a greater greenhouse effect than CO_2; measuring CO_2 produced in MFT

is confounded by abiotic (carbonate dissolution) and biogeochemical (mineral precipitation and dissolution) interactions with tailings minerals (Siddique et al., 2014), complicating measurement and modeling.

Methane production from hydrocarbons involves two microbial processes: the oxidation of labile hydrocarbons to simple organic compounds by Bacteria and the conversion of those compounds to CH_4 and CO_2 by Archaea (Fig. S2). Therefore, the model was developed in two modules. The first module (Section 2.1) comprising two systems of equations describes bacterial biodegradation of 18 hydrocarbon substrates (see Section 2.3.1 for selection rationale) and includes formation of microbial biomass. The second module (Section 2.2) considers archaeal CH_4 generation from bacterial metabolites. Model parameters unavailable in the literature were estimated by data fitting using laboratory measurements (Section 2.3). The model then was quantitatively validated by comparison (1) to measurements from independent but analogous laboratory experiments conducted using oil sands tailings incubated with whole diluents or components of naphtha or paraffinic diluents and (2) to field measurements of CH_4 emissions from OSTP (Section 2.4). Finally the model was qualitatively assessed using phase plane analysis to illustrate CH_4 emission trajectories in OSTP and EPL (Section 2.5 and supplementary material Section S3). Terms used in model development are defined in Table 1.

2.1. Biodegradation and biomass module development

Direct measurement of hydrocarbon biodegradation kinetics in OSTP and EPL is technically infeasible. Therefore this module describes the dynamics of CH_4 production from MFT incubated with cognate naphtha or paraffinic diluents under laboratory conditions analogous to those expected in OSTP or EPL. A brief description of previously published cultivation methods used to generate model data is given in supplementary material section S1.

Microbial biomass can change as a result of growth and death. Because hydrocarbon biodegradation is initiated by Bacteria and not by

Table 1
Definition of terms used in model development.

Term	Definition
C_i	Mass of individual labile hydrocarbons in the system, where $i = 1...n$, assuming n labile hydrocarbons in system[a]
C_i^{in}	Mass of C_i inflow to the system
C_T	Total mass of labile (biodegradable) hydrocarbon in the system (i.e., the sum of all C_i)
μ	Specific microbial growth rate of microbes (Bacteria and Archaea) supported by C_T
μ_i	Specific microbial growth rate supported by each labile hydrocarbon C_i
N_T	Total mass of nitrogen in the system
N_A	Mass of N_T that is biologically available[b]
B	Total biomass of living microbes
b	Biomass of dead microbes
β_i	The proportion of C_i contained in dead biomass that is available for microbial recycling
θ	The ratio of nitrogen to carbon associated with microbial biomass B
r	Proportionality constant defining efficiency of conversion of C_T to B
r_i	Proportionality constant defining efficiency of conversion of each C_i to B; r_i = B/C_i consumed
λ_i	Lag period before the onset of biodegradation of each C_i
d	Microbial cell death rate
K_f	N_A-dependent half-saturation constant
K_{gi}	C_i-dependent half-saturation constant
Γ_i	Expected yield of CH_4 from biodegradation of 1 mol of C_i
G_i	Total CH_4 and CO_2 generated from the biodegradation of C_i
η	Fraction of sum of Γ_i for all i, yielded by biodegradation of C_T; i.e., methane bioconversion efficiency factor
η_i	Fraction of Γ_i yielded by biodegradation of each C_i

[a] In developing the current model, we considered 18 specific hydrocarbons present in naphtha and paraffinic diluents (see Table 2).
[b] e.g., nitrate, nitrite, ammonium, dinitrogen (N_2 gas), labile organic N compounds (e.g., macromolecules in biomass), but not complex molecules (e.g., resins found in bitumen).

the archaeal methanogens (Fig. S2), this module considers only bacterial kinetics. The per cell bacterial growth rate is assumed to follow Liebig's law of the minimum (Sterner and Elser, 2002) stating that growth rate is proportional to the most limiting resource available. The model assumes, based on chemical analysis of oil sands tailings (Collins, 2013; Penner and Foght, 2010), that all relevant nutrients except biologically-available nitrogen (defined in Table 1) and/or labile carbon are present at non-limiting concentrations in OSTP and EPL. Therefore the bacterial growth rate is modeled as a function only of the mass of biologically-available nitrogen (N_A) and labile hydrocarbons (C_i, the mass of labile hydrocarbons in the system for $i = 1...n$, assuming n discrete labile hydrocarbons in the system). Assuming that there is negligible input of N_A with fresh tailings, no outflow of soluble N_A and no loss of gaseous NO_x, we take the total nitrogen (N_T) in these systems to be constant. With this assumption, the subset of N_T available for bacterial growth (N_A) is given by $N_A = N_T - \theta B$ where θ is the ratio of nitrogen to carbon in the total microbial biomass B, and θ is assumed to be constant (Makino et al., 2003). The Monod functions $f(N_A) = \dfrac{N_A}{N_A + K_f}$ and $g(C_i) = \dfrac{C_i}{C_i + K_{g_i}}$ are used to model the nitrogen- and carbon-dependent growth rates respectively, where K_f is the N_A-dependent half-saturation constant; K_{g_i} is the C_i-dependent half-saturation constant; and C_i^{in} is the inflow of C_i to the system. Thus, the C_i-dependent per cell bacterial growth rate μ is given by μ_i min $\{f(N_A), g(C_i)\}$, where μ_i is the maximum growth rate of Bacteria growing on only the hydrocarbon C_i present and is unique for each labile hydrocarbon. Hence the total per cell growth rate of Bacteria is $\sum_{i=1}^{n} \mu_i$ min$\{f(N_A), g(C_i)\}$.

The biodegradation rate of each labile hydrocarbon i is assumed to be proportional to the bacterial growth rate due to its consumption, i.e., [per cell bacterial growth rate due to each hydrocarbon] $\propto$ [biodegradation rate of hydrocarbon]. This implies that [the per cell bacterial growth rate supported by each labile hydrocarbon i] = r_i[the per cell biodegradation rate of that hydrocarbon] where r_i is a proportionality constant reflecting the efficiency of bacterial conversion of substrate into biomass. Hence, [the per cell biodegradation rate of each labile hydrocarbon] = $\dfrac{1}{r_i}$ [the per cell bacterial growth rate supported by labile hydrocarbons], i.e., [the per cell biodegradation rate of each hydrocarbon] = $\sum_{i=1}^{n} \dfrac{1}{r_i} \mu_i$ min$\{f(N_A), g(C_i)\}$. Archaeal growth and death are considered in the second module (Section 2.2).

We assume that microbial death rate (d) is constant in the laboratory cultures and that nutrients in dead microbial biomass are quickly recycled back into labile carbon and nitrogen (N_A). The fraction of C_i recycled from dead biomass b is assumed to be a constant β_i where $0 < \beta_i < 1$.

In accordance with laboratory observations (Mohamad Shahimin and Siddique, 2017a, 2017b; Siddique et al., 2007, 2006), the model assumes that onset of biodegradation of each hydrocarbon begins after a unique lag period, λ_i. The above assumptions lead to the following system of equations:

$$g(C_i) = \begin{cases} 0, & t < \lambda_i \\ \dfrac{C_i}{K_{g_i} + C_i}, & t \geq \lambda_i \end{cases} \quad \dfrac{dB}{dt} = B \sum_{i=1}^{n} \mu_i \ min\left\{\dfrac{N_A}{K_f + N_A}, g(C_i)\right\} - dB, \dfrac{dC_i}{dt} = \dfrac{-1}{r_i}\mu_i B min\left\{\dfrac{N_A}{K_f + N_A}, g(C_i)\right\} + \beta_i dB + C_i^{in}, N_A = N_T - \theta B, B(0) > 0, C_i(0) \geq 0. \tag{1}$$

Since the carbon- and nutrient-dependent growth efficiency parameters describe the main differences in bacterial utilization of different hydrocarbons, the model assumes that parameters such as carbon conversion efficiency, intrinsic bacterial growth rate, and carbon recycling

from dead Bacteria (negligible in our data fitting), are equivalent for different hydrocarbons; i.e., $\mu_i = \mu$, $r_i = r$, and $\beta_i = \beta$. With this assumption, the system of equations becomes:

$$g(C_i) = \begin{cases} \dfrac{C_i}{K_{g_i} + C_i}, t \geq \lambda_i \dfrac{dB}{dt} = B\sum_{i=1}^{n} \mu min\left\{\dfrac{N_A}{K_f + N_A}, g(C_i)\right\} - dB, \dfrac{0, \quad t<\lambda_i}{dC_i} \\ = \dfrac{-1}{r}\mu Bmin\left\{\dfrac{N_A}{K_f + N_A}, g(C_i)\right\} + \beta dB + C_i^{in}, N_A \end{cases} \quad (2)$$

$$= N_T - \theta B, B(0) > 0, C_i(0) \geq 0.$$

To analyze the types of solutions that this model could produce, a steady state analysis was performed. The algebraic analysis is described in supplementary material Section S2 and is of particular use because it allows solutions to be classified by parameter values.

2.2. Methane biogenesis module development

From the preceding biodegradation module, bacterial biodegradation of a hydrocarbon substrate (C_i) per unit time yields $\frac{1}{r}\mu Bmin\{\frac{N_A}{K_f + N_A}, g(C_i)\}$ units of metabolite(s) corresponding to C_i. The metabolite(s) ultimately are converted to CH_4 and CO_2 (G_i) by methanogens (Fig. S2). Since methanogens have a slow growth rate compared to that of the hydrocarbon-degrading Bacteria (being dependent on their metabolism), we assume that the biomass of methanogens in the system is constant. With these additions, the system of Eq. (2) becomes:

$$g(C_i) = \begin{cases} \dfrac{C_i}{K_{g_i} + C_i}, t \geq \lambda_i \dfrac{dB}{dt} = B\sum_{i=1}^{n} \mu min\left\{\dfrac{N_A}{K_f + N_A}, g(C_i)\right\} - dB, \dfrac{0, \quad t<\lambda_i}{dC_i} \\ = \dfrac{-1}{r}\mu Bmin\left\{\dfrac{N_A}{K_f + N_A}, g(C_i)\right\} + \beta dB + C_i^{in}, \dfrac{dG_i}{dt} \\ = \dfrac{1}{r}\mu Bmin\left\{\dfrac{N_A}{K_f + N_A}, g(C_i)\right\}, CH_4 = \sum_{i=1}^{n}\eta_i\Gamma_i G_i, N_A \end{cases} \quad (3)$$

$$= N_T - \theta B, B(0) > 0, C_i \geq 0, G_i(0) = 0$$

where, Γ_i is the maximum theoretical yield of CH_4 expected from biodegradation of one mole of C_i. This value can be calculated from Eq. (4) (derived from Symons and Buswell, 1933, as implemented by Roberts, 2002) that describes the complete oxidation of hydrocarbons to CH_4 and CO_2 under methanogenic conditions, namely:

$$C_cH_h + \left(c - \dfrac{h}{4}\right)H_2O \rightarrow \left(\dfrac{c}{2} - \dfrac{h}{4}\right)CO_2 + \left(\dfrac{c}{2} + \dfrac{h}{8}\right)CH_4 \quad (4)$$
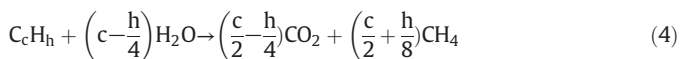
where c and h are, respectively, the numbers of carbon and hydrogen atoms in a C_i molecule.

From Eq. (4), $\Gamma_i = (\frac{c}{2} + \frac{h}{8})$. Furthermore, η_i is the fraction of the theoretical CH_4 yield from the biodegradation of a mole of C_i (i.e., a conversion efficiency factor) and is assumed to be the same for all C_i, i.e., $\eta_i = \eta$, with $0 < \eta_i < 1$. The values of η_i used in numerical simulations were obtained from (Mohamad Shahimin et al., 2016; Mohamad Shahimin and Siddique, 2017a, 2017b; Siddique et al., 2007, 2006) and Table S1.

2.3. Acquisition of laboratory data, parameter estimation and model validation

Our approach was to select a suite of 18 relevant labile hydrocarbons to generate model predictions, then estimate missing model parameters using empirical biodegradation kinetics and CH_4 measurements for

these hydrocarbons, and finally to test the stoichiometric model quantitatively using measurements from an independent set of laboratory experiments.

2.3.1. Model hydrocarbon selection and testing

Fugitive diluent in froth treatment tailings (Fig. S1) is the predominant substrate for methanogenesis in OSTP (Foght et al., 2017). The most commonly used diluents are naphtha and paraffinic solvent. Syncrude Canada Ltd. (Syncrude), Suncor, and Canadian Natural Resources Ltd. (CNRL) use naphtha, the composition of which differs slightly for each company but which comprises primarily paraffinic (n-, iso- and cyclo-alkanes) and monoaromatic hydrocarbons (predominantly toluene and three xylene isomers), typically in the C_6-C_{10} range (Siddique et al., 2008; Burkus et al., 2014). Canadian Natural Upgrading Limited (CNUL; formerly Shell Albian), Imperial (Kearl Mine) and Suncor (Fort Hills Mine) use a paraffinic diluent comprising n- and iso-alkanes primarily in the C_5–C_6 range (Mohamad Shahimin and Siddique, 2017a). Published results from laboratory experiments incubating these whole diluents or their major constituents with MFT from Syncrude, CNUL or CNRL (Mohamad Shahimin et al., 2016; Mohamad Shahimin and Siddique, 2017a, 2017b, Siddique et al., 2007, 2006; and Table S1) revealed complete or significant biodegradation of 18 hydrocarbons in neat diluents added to MFT and incubated under methanogenic conditions, including the n-alkanes n-pentane (C_5), n-hexane (C_6), n-heptane (C_7), n-octane (C_8), n-nonane (C_9), and n-decane (C_{10}); the iso-alkanes 2-methylpentane (2-MC_5), 2-methylhexane (2-MC_6), 3-methylhexane (3-MC_6), 2-methylheptane (2-MC_7), 4-methylheptane (4-MC_7), 2-methyloctane (2-MC_8), 3-methyloctane (3-MC_8) and 2-methylnonane (2-MC_9); and the monoaromatics toluene, o-xylene and m- plus p-xylenes (the latter two are not resolved by our gas chromatography column and are therefore reported as a sum). Table 2 lists the 18 labile hydrocarbons selected for model development, the source of biodegradation data, the type of tailings used to generate the data and the parameters estimated using those data.

2.3.2. Parameter estimation

The values of many model parameters in the system of Eq. (3) are not available in the literature, including the initial microbial biomass in OSTP and EPL ($B(0)$), the nitrogen half-saturation constant (K_f) and the half-saturation constants of the biodegradable hydrocarbons (K_{gi}) and λ_i. Because these parameters are related to the biodegradation module, we fit the biodegradation module (system of Eq. (2)) to data obtained from laboratory biodegradation studies cited above. To estimate these values, we used the nonlinear regression function nlinfit(.) in MATLAB, which uses the Levenberg-Marquardt algorithm (Moré, 1978), to fit the solution of the biodegradation module to the data. We provided the function with empirical data (see Table 2 for sources), the time points at which the data were collected (X), our simulated results at X, and a random initial guess of parameter values. The system was integrated by calling a function that takes as input the initial parameter values, the time at which the empirical data were collected, and for any given time X uses the MATLAB function ode15s(.) to perform the integration. The solution of the system obtained from the function was then evaluated at X, using the MATLAB function deval(.). We also estimated the 95% confidence intervals of the predicted values by using the MATLAB function nlparci(.). To achieve this, we provided this function with the coefficient estimates, residuals and the estimated coefficient covariance matrix from nlinfit(.). Some of the microbial model parameters used in the simulation, namely μ, r, and θ, were taken from the literature: the units, values and source of these parameters are provided in Table S2. We assume here that no microbes died during laboratory incubation; thus, in fitting the data to our model, we take d to be zero.

Table 2
List of 18 labile diluent hydrocarbons used in model development, sources of data and type of tailings used to generate data for the biodegradation module and to estimate model parameter values, and the model parameters estimated using those data (see Table S4 for parameter definitions and values).

Hydrocarbon	Source of data	Type of tailings	Parameters estimated from the data
n-Alkanes			
C_5	Mohamad Shahimin et al. (2016)	CNUL	K_{gC_5} and C_5-lag
C_6, C_7, C_8, C_{10}	Siddique et al. (2006)	Syncrude	B(0), K_f, N_T, K_{gC_6}, K_{gC_7}, K_{gC_8}, $K_{gC_{10}}$, C_6-lag, C_7-lag, C_8-lag and C_{10}-lag.
C_9	Table S1	Syncrude	K_{gC_9} and C_9-lag
iso-Alkanes[a]			
2-MC_6[b], 3-MC_6, 2-MC_7, 4-MC_7, 2-MC_8, 3-MC_8,[b] 2-MC_9[b]	Siddique et al., unpublished	Syncrude	K_{g3-MC_6}, K_{g2-MC_7}, K_{g4-MC_7}, K_{g2-MC_8}, 3-MC_6 –lag, 2-MC_7-lag, 4-MC_7-lag, and 2-MC_8-lag
2-MC_5	Siddique et al., 2015	CNUL	K_{g2-MC_5} and 2-MC_5-lag
Monoaromatics			
Toluene, *o*-xylene, *m*-plus *p*-xylene	Siddique et al. (2007)	Syncrude	$K_{gtoluene}$, $K_{go-xylene}$, $K_{gmp-xylene}$, toluene-lag, *o*-xylene-lag, and *m,p*-xylene-lag

[a] M denotes a methyl group; i.e., 2-MC_6 is 2-methylhexane, etc. See Methods Section 2.3.1 for full list of abbreviations.
[b] The values of model parameters K_g and lag for 2-MC_6, 3-MC_8 and 2-MC_9 are not available from empirical studies and are assumed to be the same as those for 3-MC_6, 2-MC_8 and 2-MC_8, respectively, due to their similar molecular weights.

2.3.3. Model validation against laboratory data

The new stoichiometric model was then validated against CH_4 production data generated in independent but parallel laboratory studies that measured biodegradation of paraffinic diluent in CNUL MFT (Mohamad Shahimin and Siddique, 2017a) and naphtha in Syncrude (Table S1) and CNRL MFT (Mohamad Shahimin and Siddique, 2017b). To this end, the concentrations of the labile hydrocarbons initially present in each diluent were used in the model to predict CH_4 production (Table S7). These predictions were compared with measured CH_4 produced by those tailings in independent laboratory experiments using the *goodnessOfFit(.)* function in MATLAB. As input, we provided this function with our test data, the simulated data from our model, and a cost function that determines the goodness of fit. We used the Normalized Mean Square Error (NMSE) function for this statistic, computed as

$$NMSE = 1 - \frac{\|[actual]-[predicted]\|^2}{\|[actual]-[mean\ of\ actual]\|^2},$$

where $\|.\|$ indicates the 2-norm of a vector, *predicted* is the output simulated by our model, *actual* is the input test data and *mean of actual* is the mean of the test data. $NMSE \in [-\infty, 1]$ where $-\infty$ indicates a bad fit and 1 a perfect fit.

2.4. Quantitative comparison of model prediction and in-situ measurement of CH_4 emissions from OSTP

To further validate the applicability of the new stoichiometric model for predicting in-situ CH_4 emissions, we used (1) a modeling approach where kinetics of CH_4 production were estimated to determine the duration of CH_4 emissions, and (2) a direct approach that yielded a ballpark value of potential CH_4 emissions. For both approaches, we estimated the total mass of diluent entrained in froth treatment tailings entering Syncrude MLSB, CNRL Horizon and CNUL MRM OSTPs in 2016 and 2017 (Table S6) and estimated the mass of individual biodegradable hydrocarbons in the three diluents (Table S7), using published diluent compositions. To employ the modeling approach, we assumed that these masses of individual hydrocarbons were present at the start of each year (i.e., the model was run as if all the diluent was introduced on January 1 of the year), while acknowledging the continuous input of similar amounts of diluents in the years preceding 2016. Using the estimated parameter values in Table S4, we modeled CH_4 production and calculated the predicted cumulative CH_4 produced by metabolism of the constituent hydrocarbons over 366 days. The model output was compared with cumulative CH_4 emissions measured in flux chambers at the surface of OSTP as reported to the Government of Alberta (unpublished; raw data available upon request) (Table S8). Notably, surface

flux measurements of CH_4 are not yet available for the single EPL that was established in 2013, so the current comparison is limited to OSTP measurements. In the direct approach, theoretical CH_4 production was estimated from the masses of individual hydrocarbons biodegraded to methane using stoichiometric equations as described in Table S8.

2.5. Qualitative assessment of model predictions for OSTP and EPL

In addition to quantitative analyses, the model was also qualitatively challenged to predict the trajectories of CH_4 generation from OSTP (continuous $C_i^{in}>0$) versus EPL ($C_i = 0$) under hypothetical scenarios of carbon or nitrogen availability in-situ. To ease assessment, we reduced the biodegradation module to a system of two equations by letting C_T and C_T^{in} to represent, respectively, the sum of all labile hydrocarbons in the system and C_i^{in}, and then performed a phase plane analysis of the reduced system (supplementary material section S3).

Equations were solved for microbial biomass versus total carbon content under eight combinations of C_i and N_A limitation over time.

The code is available at http://www.judekong.ca/publication/2019-05-01-Methanebiogenesismodel or from the authors upon request.

3. Results and discussion

Previous zero- and first-order CH_4 production models from oil sands tailings (Siddique et al., 2008) used the available limited experimental data for diluent biodegradation and CH_4 production from four short-chain *n*-alkanes and four monoaromatic compounds during <1 year incubation with MFT from a single OSTP (Siddique et al., 2007, 2006). Those first approximation models assumed that organic carbon was the sole limiting nutrient in-situ and that microbial biomass was constant in OSTP despite receiving continuous and consistent inputs of diluent in froth treatment tailings. The stoichiometric model described here accounts for additional parameters including recently published biodegradation kinetics and CH_4 measurements for 18 relevant hydrocarbons including additional *n*-alkanes and, for the first time, isoalkanes, incubated for much longer (up to 6.5 years) with MFT from three different OSTP impacted by distinct diluents. These additional experimental data allow the estimation of some kinetic parameters not previously considered and enable the new model to account for more biological factors than the previous models, so as to be adaptable to future modeling of in-situ CH_4 production from OSTP and EPL.

3.1. Data fitting to biodegradation and methane generation modules

The biodegradation module was evaluated by fitting system of Eq. (2) to published experimental data sets for the 18 labile

hydrocarbons listed in Table 2. Figs. S3–S5 show the simulated biodegradation of diluent n-alkanes, monoaromatics and isoalkanes compared with measured biodegradation of these components. We obtained goodness-of-fit statistics (NMSE) ranging from 0.85 to 1.00 (Table S3). These statistics show that the performance of the module with respect to the training data is good.

To integrate the methane generation module with the biodegradation module, only three model parameters were available in the literature (Table S2); others had to be estimated from experimental data (Tables 2 and S4). Using these calculated values, we applied the full stoichiometric model to methane measurements from a suite of experiments analogous to but independent of those used to estimate the parameters. Specifically, the CH_4 measurements were acquired during long-term incubation of MFT samples from Syncrude, CNUL and CNRL with their cognate diluents (Table S1, Mohamad Shahimin and Siddique, 2017a, Mohamad Shahimin and Siddique, 2017b, respectively). Fig. 1 shows that the model predicted methane generation very well for all three types of MFT over long incubation times (>4 yr incubation for CNUL and CNRL cultures). Additional modeling of Syncrude MFT with mixtures of n-alkane or monoaromatic components of its
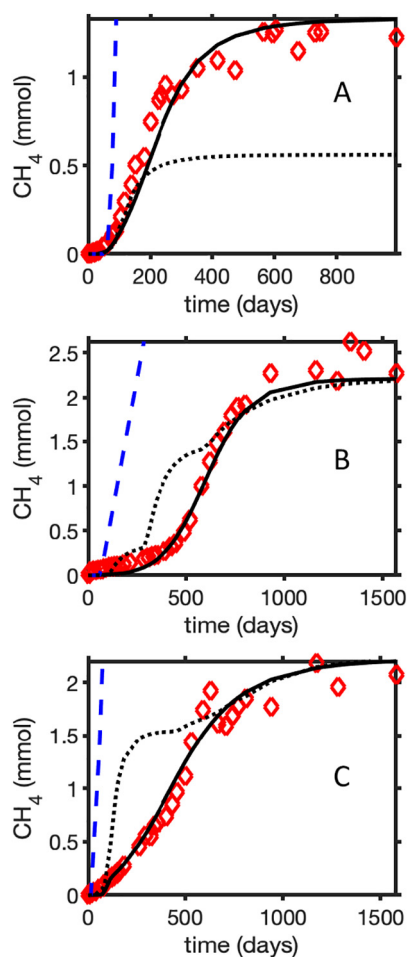
Fig. 1. Comparison of CH_4 production predicted by the stoichiometric model and previous models (Siddique et al., 2008) versus CH_4 measured in laboratory cultures independent of those used to generate the stoichiometric model and parameters (Table S4). Methane measurements (diamond symbols) are from cultures comprising: (A), Syncrude MFT incubated with its naphtha diluent; (B), CNUL MFT incubated with its paraffinic diluent; and (C), CNRL MFT incubated with its naphtha diluent. Solid lines represent the stoichiometric model prediction; dashed lines and dotted lines respectively represent predictions made by applying the previous zero-order and first-order models (Siddique et al., 2008) to the independent data set. The parameter values used in simulating the zero-order and first-order models were obtained from Siddique et al. (2008) and Table S5.

Table 3

Normalized mean square error (NMSE) analysis of model predictions and measured CH_4 production from laboratory cultures comprising three MFT samples incubated with their cognate diluents. See Figs. 1 and S6 for graphical comparison of model outputs.

	NMSE values		
	MFT source and diluent type		
	Syncrude	CNUL	CNRL
Model	Naphtha diluent	Paraffinic diluent	Naphtha diluent
Zero-order[a]	−0.28	−1.00	−1.10
First-order[a]	−0.65	0.82	0.61
Stoichiometric	0.81	0.98	0.97

[a] implemented as described by Siddique et al. (2008), using data reported in the current study.

diluent (rather than whole diluent) also showed very good methane prediction (Fig. S6).

3.2. Model evaluation and comparison to previous models

Goodness-of-fit analysis of the stoichiometric model was calculated using NMSE (Table 3) that showed excellent fit, ranging from 0.81 to 0.98 for the three combinations of MFT and diluent. These NMSE results indicate that the integrated biodegradation and CH_4 production modules rightly capture the behaviour of independent laboratory cultures and that the stoichiometric model is sufficiently flexible to accommodate different inocula and substrates over long incubation periods.

The new stoichiometric model was then compared with the previous zero- and first-order kinetic models, as performed previously (Siddique et al., 2008) but using the current data set. To this end, we first estimated the zero- and first-order kinetic model-related parameter values for the labile hydrocarbons that were not considered by Siddique et al. (2008) (Table S5). Figs. 1 and S6, and Table 3 show that the stoichiometric model provides improved predictions over the previous models for describing CH_4 biogenesis from Syncrude MFT and whole naphtha or its components, and is far superior (matching closely with the measured methane values) to the previous simpler models for the CNUL MFT–paraffinic diluent and for CNRL–naphtha combinations, neither of which were available for the earlier modeling study. The improved fit regarding lag time and extent of CH_4 production, and the improved NMSE values suggest that the stoichiometric model, which is based on laboratory cultures, would be useful for modeling in-situ CH_4 production from different OSTP and EPL.

3.3. Quantitative comparison of stoichiometric model predictions to measured cumulative CH_4 field emissions

To evaluate the feasibility of applying this model based on laboratory cultures to field emissions of CH_4, we compared the reported measured volumes of CH_4 emitted from the surfaces of OSTPs with cumulative CH_4 masses predicted by our model. Table 4 shows the comparison between the reported measured methane emissions from OSTPs in 2016 and 2017 and the maximum theoretical CH_4 yield predicted by our model based on the estimated masses of diluent entering OSTPs for 2016 and 2017 (Table S6). The stoichiometric model predictions are 50–55% of the measured emissions from Syncrude MLSB and 77–95% of the measured emissions from CNRL OSTP in both years. For CNUL where paraffinic solvent is used, the model predictions were 48% of the measured emissions in 2017 but only 17% of the emissions in 2016. This latter difference may be attributed to markedly greater methane emission data from CNUL OSTP reported in 2016 compared to all other OSTPs (Tables 4 and S5). The overall trend is very clear that the model predicted about 50% of emissions from Syncrude and CNUL OSTP and >75% of emissions from CNRL OSTP. This likely reflects the diluent compositions, with only ~40% of fugitive Syncrude and CNRL naphtha diluent being considered labile versus ~60% of CNUL paraffinic diluent,

Table 4
Comparison of cumulative field measurements of CH_4 emissions in 2016 and 2017 in three OSTP versus stochiometric model predictions of cumulative in-situ CH_4 emissions from those OSTP.

Operator and OSTP (date)	Field measurements of CH_4 emissions (moles × 10[6])[a]	Stochiometric model predictions of methane emissions (moles × 10[6])	Proportion of field emissions predicted by model (%)[b]
Syncrude MLSB (2016)	1191	656	55
Syncrude MLSB (2017)	991	492	50
CNRL Horizon (2016)	336	321	95
CNRL Horizon (2017)	599	459	77
CNUL MRM (2016)	2634	445	17
CNUL MRM (2017)	1051	506	48

[a] Unpublished surface flux measurements (Government of Alberta; raw data available upon request), reported as tonnes and converted to moles at standard temperature and pressure.
[b] For detailed calculations see Table S8.

based on the mass of known biodegradable hydrocarbons in the diluents (Table S7).

This difference between predicted and measured CH_4 masses suggests that (other than possible inaccuracies associated with field measurements) there are other endogenous carbon sources present in OSTP that support methanogenesis but are not currently accounted for by the model. Such possible sources include (but are not limited to): (1) additional labile diluent hydrocarbons not yet identified in our laboratory incubations and therefore not included in the model; (2) recalcitrant hydrocarbons deposited in previous years (and therefore not included in the annual C_i^{in} model input) that are slowly degraded as the community adapts to residual naphtha after depletion of the labile hydrocarbons in lower strata, e.g., some iso-alkanes and cycloalkanes having extremely long lag times or slow degradation rates (e.g., Abu Laban et al., 2015); (3) slowly-degradable metabolites produced historically in-situ during incomplete biodegradation of hydrocarbon or from non-hydrocarbon carbon substrates; (4) labile organic matter associated with clays in oil sands ores (Sparks et al., 2003); (5) minor labile components of bitumen e.g., high molecular weight *n*-alkanes (Oberding and Gieg, 2018); (6) organic additives used in ore processing and deposited with tailings, e.g., citrate that is used as an amendment in some OSTPs (Foght et al., 2017; Collins et al., 2016) and is a potentially large source of CH_4 in CNUL MRM; (7) the potential microbial oxidation of biogenic CH_4 either aerobically, during transition of CH_4 bubbles through the aerobic water layer on OSTP and EPL, or anaerobically in MFT. Whereas the aerobic process has been inferred in OSTP (Saidi-Mehrabad et al., 2013) and might decrease surface CH_4 emissions in the field, CH_4-consuming anaerobic methane oxidation (known to occur in some hydrocarbon-rich sediments) has not been demonstrated yet in either OSTP or in MFT cultures (Foght et al., 2017). An additional physical explanation for larger masses of measured field emissions is the delayed, stochastic release of methane produced years ago from labile HCs that is 'trapped' in lower strata of MFT (Guo, 2009) until (a) suitably-sized and -oriented channels are created (e.g., by microbial activity, Siddique et al., 2014) and/or (b) cumulative gas voids reach critical buoyancy and rise from deep tailings, and/or (c) MFT strata are disturbed by some physical activity in the pond (e.g., moving deposition pipes, transferring MFT to new pits, etc.) allowing escape of gas.

There is agreement between the model predictions and measured field emissions despite the obvious reasons for discrepancy discussed above. However, additional qualitative factors must be addressed to expand the developed model to in-situ predictions while keeping in mind the inherent differences between laboratory cultures and field operations: (1) cultures are incubated with a single input of hydrocarbons, i.e., in "batch mode" with finite C_i^{in}, whereas the upper strata of OSTP receive ongoing input of diluent, i.e., "continuous mode" where $C_i^{in} > 0$. The laboratory cultures are more analogous to EPL, where $C_i^{in} = 0$ or to the lower strata of OSTP to which fresh diluent deposited at the surface cannot effectively diffuse and where, essentially, $C_i^{in} = 0$. (2) As discussed above, anaerobic biodegradation kinetics are currently available for only 18 hydrocarbons in cultures, whereas additional constituents of whole diluent and possibly a small subset of bitumen constituents may be susceptible to biodegradation in-situ. Restriction of the parameter C_i to the current 18 hydrocarbons would likely cause the model to underestimate methane production in-situ. Selective depletion of naphtha constituents with depth in OSTP has been observed qualitatively (Fig. S2 in Foght et al., 2017) and such information could be used in future to expand the substrate range of the stoichiometric model and better represent in-situ biodegradation. (3) The diluents are added neat to MFT cultures, whereas in-situ the diluents are incorporated in bitumen globules where their biological availability may decrease and depend upon partitioning to the bitumen-water and/or bitumen-microbe interface. Alternatively, sequestration in bitumen could protect microbes from deleterious effects of solvent hydrocarbons such as monoaromatics, thus enhancing overall biodegradation. Insufficient data exist currently to argue for either possibility. (4) The model currently includes a variable for lag time (λ), the time elapsed between addition of hydrocarbon and appearance of measureable CH_4. In fact, lag times of 5–15 years were observed between the inauguration of OSTP and the first observation of ebullition at the pond surface (Foght et al., 2017), likely reflecting the time required for establishment of efficient methanogenic communities. However, this variable is likely relevant only to laboratory studies, due to disruption of the microbial consortia during initiation of the cultures, and to newly established OSTP and EPL when transfer of tailings begins. After onset of CH_4 production, OSTP subsequently do not exhibit any apparent lag phases because of continuous diluent input; therefore $\lambda = 0$ in-situ. (5) Small scale culture bottles facilitate release of CH_4 from MFT to the headspace for measurement compared with static deep strata in OSTP and EPL that experience physical retention of GHG as methane voids (Guo, 2009). That is, the model predicts CH_4 production based on 100% release from MFT; the proportion of gas released to the pond surface versus that retained under hydraulic pressure in-situ is not a component of the model. (6) Methanogenesis depends completely upon the microbial community composition, which is complex (An et al., 2013) and specific to each OSTP and EPL (Wilson et al., 2016), and may diverge from cultured communities during incubation. Although some diversity data exist both for cultures and various MFT, the model does not include parameters to account for the presence or abundance of 'keystone' microbial species because, in tailings, such species currently are incompletely known or identified. Significant efforts in research and testing would be required to integrate microbial community analysis into any CH_4 model for oil sands operations. (7) Finally, the model does not currently include parameters that reflect potential changes to ore processing or OSTP practices such as subtle alterations in diluent composition, intermittent deposition of chemicals from related processes (e.g., ammonium, citrate; Foght et al., 2017), changes in froth treatment water temperature, etc.

3.4. Qualitative test of model prediction

Despite the shortcomings of applying the model to field predictions listed above, and in anticipation of acquiring in-situ measurements to provide parameters for use in future for field modeling, it is possible to conduct a qualitative test of the stoichiometric model to determine whether it predicts expected trajectories under different expected

field scenarios, e.g., limiting C_T and/or N_A conditions. Whereas cultures receive hydrocarbons in excess of instantaneous microbial demand at the beginning of incubation, as do the upper strata of active OSTP, labile carbon may become limiting in lower (older) strata of OSTP and eventually in EPL and cultures, where diluent is not replenished. Similarly, cultures initially receive a very small but finite amount of soluble nitrogen and have a headspace of N_2 gas (which may serve as a nitrogen source for tailings microbiota; Collins et al., 2016) but the lower strata of OSTP and EPL have no obvious input of biologically available nitrogen (N_A). Therefore this nutrient (or others, currently unidentified) may become limiting with time. Thus, challenging a model developed using culture data with scenarios reflecting in-situ conditions should reveal the strength of the model. Phase plane analyses of eight forms of potential solutions of the stoichiometric model are shown in Figs. S7 and S8 and described in supplementary material section S3. The model outputs describe the expected trajectories of OSTP and EPL under carbon and/or nitrogen limitation, solving for biomass and total carbon in the system with time, i.e., the sum of all microbial activity in-situ. The predicted behaviour of OSTP with continuous diluent input differs from EPL with no additional hydrocarbon input, and the effect of limiting nutrient (nitrogen) also changes the ultimate endpoints of biomass and carbon in the two scenarios. These outputs qualitatively support the validity of the model as well as indicating that the stoichiometric model could be used to predict specific OSTP and EPL behaviour, to predict the volumes of 'legacy' CH_4 from OSTP and long-term duration of CH_4 production in-situ (particularly from EPL), and to influence decisions about oil sands reclamation strategies. If additional in-situ model parameters are acquired, the model can be further refined to improve predictive power.

4. Conclusions

The stoichiometric model represents a significant advance over previous zero- and first-order kinetic models, particularly because it predicts well the GHG emissions from different operators' OSTP using distinct diluents that may support different rates of CH_4 production or may ultimately generate greater CH_4 emissions. Application of the model to in-situ CH_4 production is still hampered by limited experimental data and field measurements; some of these gaps may be alleviated as relevant in-situ data are acquired and when future anaerobic studies provide both evidence for susceptibility of additional hydrocarbons to biodegradation and more precise values for model parameters. The model is sufficiently flexible that additional parameters can be incorporated into the modules as laboratory or field data become available. Until such time, the stoichiometric model should assist regulators and oil sands operators in qualitatively assessing long-term GHG emissions from oil sands tailings deposits and EPL reclamation sites.

Disclaimer

The Government of Alberta neither approves nor disapproves this publication.

Appendix A. Supplementary data

Supplementary data to this article can be found online at https://doi.org/10.1016/j.scitotenv.2019.133645.

References

Abu Laban, N., Dao, A., Semple, K., Foght, J., 2015. Biodegradation of C_7 and C_8 iso-alkanes under methanogenic conditions. Environ. Microbiol. 17, 4898–4915.

AER, 2019a. Alberta energy regulator ST53: Alberta in situ oil sands production summary [WWW document]. URL. https://aer.ca/providing-information/data-and-reports/statistical-reports/st53 (accessed 17 July 2019).

AER, 2019b. Alberta energy regulator homepage [WWW document]. URL. https://www.aer.ca (accessed 17 July 2019).

Alberta Greenhouse Gas Report, 2016. Alberta Greenhouse Gas Reporting Program 2012 Facility Emissions. [WWW Document]. URL. https://open.alberta.ca/dataset/9b11d727-06be-4ade-9ad9-cfea1a559103/resource/43aeec2e-b22f-4cf4-9e1b-561aad633ee8/download/2012reportgreenhousegasemissions-sep2016.pdf, Accessed date: 2 May 2019.

An, D., Caffrey, S.M., Soh, J., Agrawal, A., Brown, D., Budwill, K., Dong, X., Dunfield, P.F., Foght, J., Gieg, L.M., Hallam, S.J., Hanson, N.W., He, Z., Jack, T.R., Klassen, J., Konwar, K.M., Kuatsjah, E., Li, C., Larter, S., Leopatra, V., Nesbø, C.L., Oldenburg, T., Pagé, A.P., Ramos-Padron, E., Rochman, F.F., Saidi-Mehrabad, A., Sensen, C.W., Sipahimalani, P., Song, Y.C., Wilson, S., Wolbring, G., Wong, M.-L., Voordouw, G., 2013. Metagenomics of hydrocarbon resource environments indicates aerobic taxa and genes to be unexpectedly common. Environ. Sci. Technol. 47, 10708–10717. https://doi.org/10.1021/es4020184.

Burkus, Z., Wheler, J., Pletcher, S., 2014. GHG emissions from oil sands tailings ponds: overview and modelling based on fermentable substrates. November 2014 [WWW Document]. Alberta Environment and Sustainable Resource Deveevelopment https://era.library.ualberta.ca/items/411947ce-1a33-42d5-a2cf-172fba9a2553#.WPELKBLyvm0, Accessed date: 17 July 2019.

Charette, T., Castendyk, D., Hrynyshyn, J., Kupper, A., McKenna, G., Mooder, B., 2012. End Pit Lakes Guidance Document 2012. Cumulative Environmental Management Association Fort McMurray, Alberta, Canada vol. 2010. http://library.cemaonline.ca/ckan/dataset/2010-0016/resour ce/1632ce6e-d1a0-441a-a026-8a839f1d64bc (accessed 4.28.19).

Collins, C.E.V., 2013. Methane Production in Oil Sands Tailings Under Nitrogen-Depleted Conditions. Master's thesis. University of Alberta (accessed 17 July 2019). https://doi.org/10.7939/R36Q1SR4N.

Collins, C.E.V., Foght, J.M., Siddique, T., 2016. Co-occurrence of methanogenesis and N_2 fixation in oil sands tailings. Sci. Total Environ. 565, 306–312.

Foght, J.M., Gieg, L.M., Siddique, T., 2017. The microbiology of oil sands tailings: past, present, future. FEMS Microbiol. Ecol. 93 (5), fix034. https://doi.org/10.1093/femsec/fix034.

Government of Alberta, 2019. Electronic Resource About Oil Sands. [WWW Document]. URL. https://www.energy.alberta.ca/OS/AOS/Pages/default.aspx, Accessed date: 24 April 2019.

Guo, C., 2009. Rapid Densification of the Oil Sands Mature Fine Tailings (MFT) by Microbial Activity. PhD thesis. University of Alberta (accessed 17 July 2019). https://doi.org/10.7939/R3K988.

Makino, W., Cotner, J.B., Sterner, R.W., Elser, J.J., 2003. Are bacteria more like plants or animals? Growth rate and resource dependence of bacterial C:N:P stoichiometry. Funct. Ecol. 17, 121–130.

Mohamad Shahimin, M.F., Siddique, T., 2017a. Methanogenic biodegradation of paraffinic solvent hydrocarbons in two different oil sands tailings. Sci. Total Environ. 583, 115–122.

Mohamad Shahimin, M.F., Siddique, T., 2017b. Sequential biodegradation of complex naphtha hydrocarbons under methanogenic conditions in two different oil sands tailings. Environ. Pollut. 221, 398–406.

Mohamad Shahimin, M.F., Foght, J.M., Siddique, T., 2016. Preferential methanogenic biodegradation of short-chain *n*-alkanes by microbial communities from two different oil sands tailings ponds. Sci. Total Environ. 553, 250–257.

Moré, J.J., 1978. The Levenberg-Marquardt algorithm: implementation and theory. In: Watson, G.A. (Ed.), Numerical Analysis. Lecture Notes in Mathematics 630. Springer, pp. 105–116.

Oberding, L.K., Gieg, L.M., 2018. Methanogenic paraffin biodegradation: alkylsuccinate synthase gene quantification and dicarboxylic acid production. Appl. Environ. Microbiol. 84 (1). https://doi.org/10.1128/AEM.01773-17 (e01773-17).

Penner, T.J., Foght, J.M., 2010. Mature fine tailings from oil sands processing harbour diverse methanogenic communities. Can. J. Microbiol. 56, 459–470. https://doi.org/10.1139/W10-029.

Risacher, F.F., Morris, P.K., Arriagaa, D., Goada, C., Colenbrander Nelson, T., Slater, G.F., Warren, L.A., 2018. The interplay of methane and ammonia as key oxygen consuming constituents in early stage development of Base Mine Lake, the first demonstration oil sands pit lake. Appl. Geochem. 93, 49–59. https://doi.org/10.1016/j.apgeochem.2018.03.013.

Roberts, D.J., 2002. Methods for assessing anaerobic biodegradation potential. In: Hurst, C.J., Crawford, R.L., Knudson, G.R., McInerney, M.J., Stetzenbach, L.D. (Eds.), Manual of Environmental Microbiology, second ed ASM Press, USA, pp. 1008–1017.

Saidi-Mehrabad, A., He, Z., Tamas, I., Sharp, C.E., Brady, A.L., Rochman, F.F., Bodrossy, L., Abell, G.C.J., Penner, T., Dong, X., Sensen, C.W., Dunfield, P.F., 2013. Methanotrophic bacteria in oilsands tailings ponds of northern Alberta. ISME J 7, 908–921.

Siddique, T., Fedorak, P.M., Foght, J.M., 2006. Biodegradation of short-chain *n*-alkanes in oil sands tailings under methanogenic conditions. Environ. Sci. Technol. 40, 5459–5464.

Siddique, T., Fedorak, P.M., MacKinnon, M.D., Foght, J.M., 2007. Metabolism of BTEX and naphtha compounds to methane in oil sands tailings. Environ. Sci. Technol. 41, 2350–2356.

Siddique, T., Gupta, R., Fedorak, P.M., MacKinnon, M.D., Foght, J.M., 2008. A first approximation kinetic model to predict methane generation from an oil sands tailings settling basin. Chemosphere 72, 1573–1580.

Siddique, T., Penner, T., Semple, K., Foght, J.M., 2011. Anaerobic biodegradation of longer-chain *n*-alkanes coupled to methane production in oil sands tailings. Environ. Sci. Technol. 45, 5892–5899.

Siddique, T., Kuznetsov, P., Kuznetsova, A., Arkell, N., Young, R., Li, C., Guigard, S., Underwood, E., Foght, J.M., 2014. Microbially-accelerated consolidation of oil sands tailings. Pathway I: changes in porewater chemistry. Front. Microbiol. 5, 106. https://doi.org/10.3389/fmicb.2014.00106.

Siddique, T., Mohamad Shahimin, M.F., Zamir, S., Semple, K., Li, C., Foght, J.M., 2015. Long-term incubation reveals methanogenic biodegradation of C_5 and C_6 iso-alkanes in oil sands tailings. Environ. Sci. Technol. 49, 14732–14739.

Siddique, T., Stasik, S., Mohamad Shahimin, M.F., Wendt-Potthoff, K., 2018. Microbial communities in oil sands tailings: their implications in biogeochemical processes and tailings management. In: McGenity, T.J. (Ed.), Microbial Communities Utilizing Hydrocabons and Lipids: Members, Metagenomics and Ecophysiology. Handbook of Hydrocarbon and Lipid Microbiology, 2nd edn Springer, Cham, pp. 1–33.

Sparks, B.D., Kotlyar, L.S., O'Carroll, J.B., Chung, K.H., 2003. Athabasca oil sands: effect of organic coated solids on bitumen recovery and quality. J. Pet. Sci. Eng. 39, 417–430.

Sterner, R.W., Elser, J.J., 2002. Ecological Stoichiometry: The Biology of Elements From Molecules to the Biosphere. Princeton University Press.

Symons, G.E., Buswell, A.M., 1933. The methane fermentation of carbohydrates. J. Am. Chem. Soc. 55, 2028–2036.

Wilson, S.L., Li, C., Ramos-Padrón, E., Nesbø, C., Soh, J., Sensen, C.W., Voordouw, G., Foght, J., Gieg, L.M., 2016. Oil sands tailings ponds harbour a small core prokaryotic microbiome and diverse accessory communities. J. Biotechnol. 235, 187–196. https://doi.org/10.1016/j.jbiotec.2016.06.030.